Mon. Not. R. Astron. Soc. **365,** 447–453 (2006) doi:10.1111/j.1365-2966.2005.09689.x

New stellar members of the Coma Berenices open star cluster

S. L. Casewell,⋆ R. F. Jameson and P. D. Dobbie
Department of Physics and Astronomy, University of Leicester, University Road, Leicester LE1 7RH

Accepted 2005 September 26. Received 2005 September 16; in original form 2005 July 20

ABSTRACT

We present the results of a survey of the Coma Berenices open star cluster (Melotte 111), undertaken using proper motions from the USNO-B1.0 (United States Naval Observatory) and photometry from the Two-Micron All-Sky Survey (2MASS) Point Source catalogues. We have identified 60 new candidate members with masses in the range $1.007 < M < 0.269\,\mathrm{M}_{\odot}$. For each we have estimated a membership probability by extracting control clusters from the proper motion vector diagram. All 60 are found to have greater than 60 per cent probability of being members, more than doubling the number of known cluster members. The new luminosity function for the cluster peaks at bright magnitudes, but is rising at $K \approx 12$, indicating that it is likely that lower mass members may exist. The mass function also supports this hypothesis.

Key words: open clusters and associations: individual: Coma Berenices – open clusters and associations: individual: Melotte 111.

1 INTRODUCTION

During the last two decades there have been numerous deep surveys of young nearby open clusters focusing on the detection of very low-mass stellar and substellar members (e.g. Jameson & Skillen 1989; Lodieu et al. 2005). Since these objects fade during their evolution, in these environments they are comparatively luminous, placing them comfortably within the reach of 2/4-m-class telescopes. Furthermore, numerical simulations suggest that in clusters with ages less than ∼200 Myr, dynamical evolution should not yet have led to the evaporation of a large proportion of these members (e.g. de la Fuente Marcos & de la Fuente Marcos 2000).

For these same reasons, there have been relatively few searchs of this type undertaken in older open clusters. Indeed, the few deep, large-area surveys of the Hyades, the most extensively studied cluster of its type and the closest to the Sun (46.3 pc: Perryman et al. 1998), have led to the identification of only a very small number of low-mass stellar and substellar members (e.g. Reid 1993; Gizis, Reid & Monet 1999; Moraux, private communication). This finding is loosely in agreement with the predictions of *N*-body simulations which indicate that less than one-fifth of the original population of substellar members remains tidally bound to a cluster at the age of the Hyades, 625 ± 50 Myr (Perryman et al. 1998). However, despite this rough consistency, until the very low-mass populations of more open clusters of similar age to the Hyades have been studied, it seems premature to exclude completely other interpretations for the deficit of low-mass members here, e.g. differences in the initial mass function. Furthermore, additional investigations of this nature may also be of use in refining *N*-body simulations.

Therefore we have recently embarked on a survey of the Coma Berenices open star cluster (Melotte 111, RA = $12^{\mathrm{h}}23^{\mathrm{m}}00^{\mathrm{s}}$, Dec. = $+26^{\circ}00'00''$, J2000.0) to extend our knowledge of its luminosity function towards the hydrogen-burning limit. At first glance this seems a prudent choice of target. It is the second closest open cluster to the Sun. *Hipparcos* measurements place it at $d = 89.9 \pm 2.1$ pc (van Leeuwen 1999), in agreement with older ground-based estimates (e.g. $d = 85.4 \pm 4.9$ pc: Nicolet 1981). Furthermore, foreground extinction along this line of sight is low, $E(B-V) \approx 0.006 \pm 0.013$ (Nicolet 1981). The metallicity of the cluster is relatively well constrained. Spectroscopic examination of cluster members reveals it to be slightly metal-poor with respect to the Sun. For example, Cayrel de Strobel (1990) determines $[\mathrm{Fe/H}] = -0.065 \pm 0.021$ using a sample of eight F-, G- and K-type associates, whereas Friel & Boesgaard (1992) determine $[\mathrm{Fe/H}] = -0.052 \pm 0.047$ from 14 F and G dwarf members. While estimates of the age of Melotte 111 vary considerably from 300 Myr to 1 Gyr (e.g. Tsvetkov 1989), more recent determinations, based on fitting model isochrones to the observed cluster sequence, are bunched around 400–500 Myr (e.g. Bounatiro & Arimoto 1993; Odenkirchen, Soubiran & Colin 1998). Thus the Coma Berenices open cluster is probably marginally younger than the Hyades.

However, Melotte 111 is projected over a large area of sky (∼100 deg^2) and contains considerably fewer bright stellar members than the Hyades. For example, Odenkirchen et al. (1998) determines the cluster tidal radius to be ∼5–6 pc but finds only 34 kinematic members down to $V = 10.5$ within a circular area of radius 5° centred on the cluster. He estimates the total mass of Melotte 111 to lie in the range 30–90 $\mathrm{M}_{\odot}$, which can be compared with estimates of 300–460 $\mathrm{M}_{\odot}$ for the mass of the Hyades (e.g. Oort 1979; Reid 1992). Additionally, the small proper motion ($\mu_{\alpha} = -11.21 \pm 0.26$ mas yr^{-1}, $\mu_{\delta} = -9.16 \pm 0.15$ mas yr^{-1}: van Leeuwen 1999) means that proper motion alone is not a suitable means by which to discriminate the members of Melotte 111 from the general field population. Fortunately, the convergent point for the cluster is sufficiently

⋆E-mail: slc25@star.le.ac.uk

distant at RA = $6^h40^h31\overset{s}{.}2$, Dec = $-41^\circ33'00''$ (J2000) (Madsen, Dravins & Lindgren 2002) that we can expect all the cluster members to have essentially the same proper motion.

In the first detailed survey of Melotte 111, Trumpler (1938) used proper motion, spectrophotometric and radial velocity measurements to identify 37 probable members, photometric magnitude $m_P < 10.5$, in a circular region of 7° diameter centred on the cluster. A significant additional number of fainter candidate members were identified by Artyukhina (1955) from a deep ($m_P < 15$) proper motion survey of ∼7 deg^2 of the cluster. Argue & Kenworthy (1969) performed a photographic *UBVI* survey of a circular field, $3\overset{\circ}{.}3$ in diameter, to a limiting depth of $m_P = 15.5$. They rejected all but two of Artyukhina's candidates with $m_P > 11$ but identified a further two faint objects with photometry and proper motion which they deemed to be consistent with cluster membership. Subsequently, Deluca & Weis (1981) obtained photoelectric photometry for 88 objects ($V > 11$), drawn from these two studies. They concluded that only four stars, three of which were listed by Argue & Kenworthy as probable members, had photometry and astrometry consistent with association with Melotte 111.

More recently, Bounatiro & Arimoto (1993) have searched an area of 6° × 6° centred on Melotte 111, using the Astronomische Gesellschaft Katalog 3 (AGK3) catalogue, and have identified 17 new candidate members ($m_P < 12$). However, despite Randich, Schmitt & Prosser (1996) identifying 12 new potential low-mass members ($V \approx 11.5$–16) from a *ROSAT* Position Sensitive Proportional Counter (PSPC) survey of the cluster, a detailed follow-up study has concluded that none of these is an associate of Melotte 111 (Garcia-Lopez et al. 2000). Odenkirchen et al. (1998) have used the *Hipparcos* and ACT reference catalogues to perform a comprehensive kinematic and photometric study of 1200 deg^2 around the cluster centre complete to a depth of $V \approx 10.5$. They find a total of ∼50 kinematic associates which appear to be distributed in a core–halo system. The core, which is elliptical in shape with a semi-major axis of $1\overset{\circ}{.}6$, is dominated by the more massive members, while the halo contains proportionately more low-mass associates. Odenkirchen, Soubiran & Colin also find evidence of an extra-tidal 'moving group' located in front of the cluster in the context of its motion around the Galaxy. However, from a subsequent spectroscopic study, Ford et al. (2001) conclude that approximately half of the moving group were not associated with the cluster.

The ready availability of high-quality astrometric and photometric survey catalogues [e.g. USNO-B1.0 (United States Naval Observatory), the Two-Micron All-Sky Survey (2MASS)] have made a new deeper, wide-area survey of the Coma Berenices open star cluster a tractable undertaking. In this paper we report on our efforts to use the USNO-B1.0 and 2MASS Point Source catalogues to search for further candidate low-mass members of Melotte 111. We identify 60 new candidates with proper motions and photometry consistent with cluster membership. State-of-the-art evolutionary models indicate that some of these objects have masses of only $M \approx 0.269\,M_\odot$.

2 THE PRESENT SURVEY

In ideal cases, membership of nearby open clusters can be ascertained by either photometry or proper motion. In the former approach, associates of a cluster are generally identified by insisting that they have magnitudes and colours that, within uncertainties, sit them on or close to an appropriate model isochrone (e.g. Bouvier et al. 1998). In the latter approach, as measurement errors usually dominate over the cluster velocity dispersion, selection of members simply requires that objects have astrometric motions consistent with known associates of a cluster. When combined, these two methods can yield candidates with a very high probability of cluster membership (e.g. Moraux, Bouvier & Stauffer 2001).

However, as discussed in Section 1, the proper motion of Melotte 111 is comparatively small and not suitable alone for the discrimination of cluster members. For example, members of the Pleiades open cluster, which can be readily identified astrometrically, have proper motions of $\mu_\alpha = 19.14 \pm 0.25$ mas yr^{-1}, $\mu_\delta = -45.25 \pm 0.19$ mas yr^{-1} (van Leeuwen 1999). Nevertheless, because of the large epoch difference of approximately 50 yr between the two Palomar Sky Surveys, if we restrict the search to $R < 18.0$, the proper motion measurements available in the USNO-B1.0 catalogue are sufficiently accurate that they can be used in conjunction with suitable photometry to identify candidates with a substantial probability of being members of Melotte 111. In principle the USNO-B1.0 catalogue provides B, R and I photometry, but the significant uncertainties in the photographic magnitudes (∼0.3 mag) severely limit its usefulness for this work (Monet et al. 2003). Therefore, to complement the astrometry, we choose to use J, H and K_S photometry from the 2MASS Point Source Catalogue which has signal-to-noise ratio $\gtrsim$10 down to $J = 15.8$, $H = 15.1$ and $K_S = 14.3$ (Skrutskie et al. 1997).

The survey was conducted as follows.

(i) A circular area of radius 4° centred on the cluster was extracted from the USNO-B1.0 catalogue.

(ii) Stars were selected according to the criterion $(\mu_\alpha - X)^2 + (\mu_\delta - Y)^2 < 100$, where $X = -11.21$ and $Y = -9.16$, i.e. to lie within 10 mas yr^{-1} of the *Hipparcos*-determined value for the proper motion of Melotte 111. This procedure was initially repeated for $X = -11.21$, $Y = +9.16$ and $X = +11.21$, $Y = -9.16$, to obtain two control samples (see Fig. 1). Two more control samples were later extracted from two further circular regions of USNO-B1.0 data. These data had a similar Galactic latitude to the cluster but were offset by 10° from the centre of Melotte 111. Stars were selected from these latter regions by applying the first proper motion criterion above. The known members have errors, or velocity dispersions amounting to about ±2.0 km s^{-1} (Odenkirchen et al. 1998). This corresponds to a proper motion of ±4.8 mas yr^{-1}, and the USNO-B1.0 catalogue astrometry errors (see Tables 1 and 2) are small – typically less than ±5 mas yr^{-1} for our stars. Note that

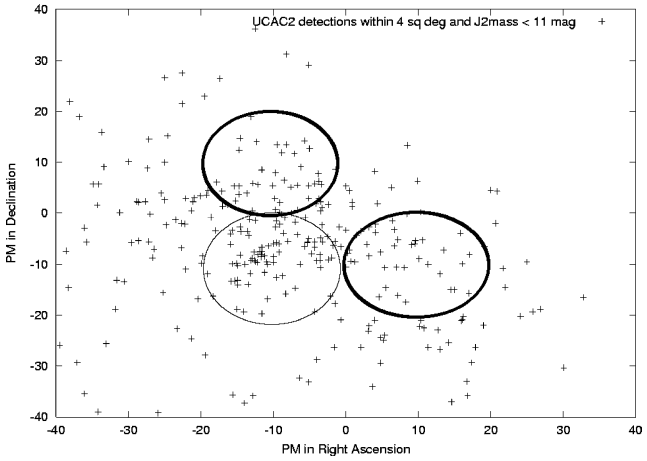

Figure 1. Plot of the USNO CCD Astronomy Catalog (UCAC; Zacharias et al. 2004) proper motions for 4 deg^2 of the cluster centre. The thin line borders the cluster proper motion selection, and the thick line borders the controls.The shallower UCAC catalogue is used here for illustration as the USNO-B1.0 catalogue only provides quantized values of 2 mas yr^{-1}.

Table 1. Name, coordinates, proper motion measurements, R, I, J, H and K_S magnitudes for the known cluster members as detailed in Bounatiro & Arimoto (1993) and Odenkirchen et al. (1998) for the area that we surveyed. The masses were calculated by linearly interpolating the models of Girardi et al. (2002) for $M \geqslant 1\,M_\odot$ or Baraffe et al. (1998) for $M < 1\,M_\odot$.

Name	RA	Dec.	μ_α	μ_δ	error μ_α	error μ_δ	R	I	J	H	K_S	Mass
	J2000.0				mas yr^{-1}							$M_\odot$
BD+26 2337	12 22 30.31	+25 50 46.1	−12.0	−10.0	0.0	0.0	4.54	4.28	3.78	3.40	3.23	2.709
BD+28 2156	12 51 41.92	+27 32 26.5	−10.0	−10.0	0.0	0.0	4.55	4.20	3.62	3.36	3.26	2.709
BD+28 2115	12 26 24.06	+27 16 05.6	−14.0	−10.0	0.0	0.0	4.79	4.65	4.40	4.23	4.14	2.685
BD+24 2464	12 29 27.04	+24 06 32.1	−18.0	0.0	0.0	0.0	5.25	5.02	4.86	4.57	4.54	2.595
BD+27 2134	12 26 59.29	+26 49 32.5	−14.0	−10.0	0.0	0.0	4.91	4.88	4.79	4.72	4.64	2.568
BD+26 2344	12 24 18.53	+26 05 54.9	−14.0	−14.0	0.0	0.0	5.11	5.08	4.93	4.94	4.89	2.496
BD+25 2517	12 31 00.56	+24 34 01.8	−12.0	−10.0	0.0	0.0	5.41	5.39	5.29	5.30	5.26	2.363
BD+26 2354	12 28 54.70	+25 54 46.2	−24.0	−16.0	0.0	0.0	5.24	5.28	5.22	5.29	5.28	2.356
HD 105805	12 10 46.09	+27 16 53.4	−12.0	−12.0	0.0	0.0	5.92	5.86	5.65	5.66	5.60	2.216
BD+26 2345	12 24 26.79	+25 34 56.8	−14.0	−14.0	0.0	0.0	6.59	6.46	5.84	5.77	5.73	2.150
BD+23 2448	12 19 19.19	+23 02 04.8	−14.0	−10.0	0.0	0.0	6.14	6.04	5.94	5.96	5.90	2.057
BD+26 2326	12 19 02.02	+26 00 30.0	−14.0	−10.0	0.0	0.0	6.36	6.27	6.08	6.00	5.98	2.018
BD+25 2523	12 33 34.21	+24 16 58.7	−12.0	−10.0	0.0	0.0	6.19	6.13	6.03	5.98	5.98	2.014
BD+27 2138	12 28 38.15	+26 13 37.0	−16.0	−8.0	0.0	0.0	6.40	6.30	6.13	6.02	5.99	2.011
BD+26 2343	12 24 03.46	+25 51 04.4	−14.0	−10.0	0.0	0.0	6.59	6.47	6.17	6.07	6.05	1.978
BD+26 2353	12 28 44.56	+25 53 57.5	−22.0	−18.0	0.0	0.0	6.52	6.40	6.16	6.10	6.05	1.977
BD+29 2280	12 19 50.62	+28 27 51.6	−12.0	−10.0	0.0	0.0	6.52	6.42	6.20	6.19	6.13	1.931
BD+26 2352	12 27 38.36	+25 54 43.5	−14.0	−12.0	0.0	0.0	6.57	6.48	6.28	6.22	6.22	1.879
BD+30 2287	12 31 50.55	+29 18 50.9	−12.0	−10.0	0.0	0.0	7.37	7.20	6.84	6.74	6.65	1.607
BD+25 2495	12 21 26.74	+24 59 49.2	−12.0	−10.0	0.0	0.0	7.23	7.08	6.79	6.74	6.66	1.600
BD+26 2347	12 25 02.25	+25 33 38.3	−14.0	−8.0	0.0	0.0	7.83	7.55	7.05	6.85	6.76	1.540
BD+26 2323	12 17 50.90	+25 34 16.8	−12.0	−12.0	0.0	0.0	7.66	7.47	7.08	6.98	6.92	1.451
BD+26 2321	12 16 08.37	+25 45 37.3	−12.0	−10.0	0.0	0.0	7.87	7.66	7.23	7.11	7.03	1.399
BD+28 2087	12 12 24.89	+27 22 48.3	−12.0	−12.0	0.0	0.0	7.85	7.64	7.27	7.13	7.08	1.380
BD+28 2095	12 16 02.50	+28 02 55.2	−24.0	−6.0	0.0	0.0	8.03	7.80	7.41	7.22	7.20	1.331
BD+27 2129	12 25 51.95	+26 46 36.0	−14.0	−10.0	0.0	0.0	8.09	7.86	7.41	7.30	7.20	1.331
BD+27 2122	12 23 41.00	+26 58 47.7	−14.0	−10.0	0.0	0.0	8.10	7.87	7.46	7.33	7.25	1.313
BD+23 2447	12 18 36.17	+23 07 12.2	−14.0	−10.0	0.0	0.0	8.39	8.13	7.63	7.38	7.30	1.294
BD+28 2109	12 21 56.16	+27 18 34.2	−10.0	−12.0	0.0	0.0	8.22	7.96	7.56	7.39	7.32	1.285
HD 107685	12 22 24.75	+22 27 50.9	−12.0	−10.0	0.0	0.0	8.23	8.00	7.60	7.39	7.38	1.263
BD+24 2457	12 25 22.49	+23 13 44.7	−14.0	−10.0	0.0	0.0	8.30	8.06	7.64	7.48	7.39	1.261
BD+28 2125	12 31 03.09	+27 43 49.2	−16.0	−8.0	0.0	0.0	8.27	8.01	7.61	7.46	7.40	1.256
BD+25 2488	12 19 28.35	+24 17 03.2	−12.0	−12.0	0.0	0.0	8.69	8.40	7.86	7.55	7.49	1.224
HD 109483	12 34 54.29	+27 27 20.2	−12.0	−10.0	0.0	0.0	8.67	8.40	7.89	7.58	7.51	1.217
BD+25 2486	12 19 01.47	+24 50 46.1	−12.0	−10.0	0.0	0.0	8.53	8.27	7.83	7.55	7.53	1.207
BD+27 2130	12 26 05.48	+26 44 38.3	−8.0	−14.0	0.0	0.0	9.44	9.04	8.13	7.68	7.58	1.193
HD 107399	12 20 45.56	+25 45 57.1	−12.0	−8.0	0.0	0.0	8.68	8.42	7.97	7.74	7.65	1.171
BD+26 2340	12 23 08.39	+25 51 04.9	−12.0	−10.0	0.0	0.0	8.80	8.52	8.02	7.76	7.68	1.160
BD+25 2511	12 29 40.92	+24 31 14.6	−10.0	−10.0	0.0	0.0	9.26	8.80	8.20	7.84	7.72	1.148
BD+27 2121	12 23 41.82	+26 36 05.3	−16.0	−12.0	0.0	0.0	8.85	8.49	8.13	7.79	7.73	1.143
BD+27 2117	12 21 49.02	+26 32 56.7	−12.0	−8.0	0.0	0.0	8.89	8.57	8.21	7.86	7.85	1.109
TYC1991-1087-1	12 27 48.29	+28 11 39.8	−12.0	−10.0	0.0	0.0	9.26	8.94	8.43	8.05	8.05	1.051
HD 105863	12 11 07.38	+25 59 24.6	-12.0	-10.0	0.0	0.0	9.14	8.84	8.38	8.11	8.07	1.043
BD+30 2281	12 29 30.02	+29 30 45.8	10.0	0.0	0.0	0.0	9.41	9.12	8.38	8.16	8.07	1.043
BD+28 2119	12 28 21.11	+28 02 25.9	−14.0	−12.0	0.0	0.0	9.92	9.54	8.94	8.47	8.46	0.915

the USNO-B1.0 proper motion errors are quantized in units of 1 mas yr^{-1}, and a zero error thus indicates an error of less than 0.5 mas yr^{-1}. Thus if we select a bounding circle of 10 mas yr^{-1}, and the total quadratically added error is 7 mas yr^{-1}, we have selected all stars to a completeness level of 1.4σ, which means that our survey is complete to ≈90 per cent.

(iii) Stars passing the above sets of criteria were cross-referenced against the 2MASS Point Source Catalogue using a match radius of 2 arcsec.

(iv) Subsequently the sample of candidate cluster members and the four control samples were plotted in $J - K_S$, K_S colour–magnitude diagrams (CMDs) as illustrated in Fig. 2 (top and bottom panels respectively).

A cursory glance at the CMDs in Fig. 2 reveals that our method appears to be rather successful in finding new associates of Melotte 111. An obvious cluster sequence can be seen extending to $K \approx 12$, beyond which it is overwhelmed by field star contamination. To perform a quantitative selection of candidate members we restrict ourselves to $K_S < 12$. We use as a guide to the location of the cluster sequence the previously known members and a 400-Myr NEXTGEN isochrone for solar metallicity (Baraffe et al. 1998), scaled to the *Hipparcos* distance determination for Melotte 111. In

Table 2. Coordinates, proper motion measurements, R, I, J, H and K_S magnitudes, mass calculated from linearly interpolating the NEXTGEN model and the absolute K_S magnitude, and the probability of membership for each of our 60 possible members.

RA	Dec.	μ_α	μ_δ	error μ_α	error μ_δ	R	I	J	H	K_S	Mass	Membership
J2000.0		mas yr^{-1}									$M_\odot$	probablility
12 24 17.15	+24 19 28.4	−18.0	−14.0	0.0	0.0	9.44	9.08	8.42	7.95	7.90	0.880	0.64
12 38 14.94	+26 21 28.1	−6.0	−2.0	0.0	0.0	9.57	9.13	8.56	8.07	8.00	0.836	0.64
12 23 28.69	+22 50 55.8	−14.0	−10.0	0.0	0.0	9.77	9.23	8.60	8.09	8.01	0.815	0.64
12 31 04.78	+24 15 45.4	−8.0	−4.0	0.0	0.0	9.76	9.19	8.81	8.28	8.20	0.798	0.79
12 27 06.26	+26 50 44.5	−12.0	−8.0	0.0	0.0	9.59	9.31	8.64	8.33	8.25	1.007	0.94
12 27 20.69	+23 19 47.5	−14.0	−10.0	0.0	0.0	9.83	9.46	8.91	8.54	8.45	0.936	0.64
12 23 11.99	+29 14 59.9	−2.0	−6.0	0.0	0.0	10.29	9.84	9.13	8.58	8.47	0.764	0.79
12 33 30.19	+26 10 00.1	−16.0	−10.0	0.0	0.0	10.59	10.14	9.24	8.72	8.59	0.766	0.79
12 39 52.43	+25 46 33.0	−20.0	−8.0	0.0	0.0	10.79	10.49	9.23	8.74	8.65	0.824	0.64
12 28 56.43	+26 32 57.4	−14.0	−8.0	0.0	0.0	10.53	10.25	9.21	8.77	8.66	0.852	0.64
12 24 53.60	+23 43 04.9	−4.0	−8.0	0.0	0.0	10.73	10.34	9.39	8.86	8.82	0.840	0.64
12 28 34.29	+23 32 30.6	−8.0	−14.0	0.0	0.0	10.40	9.97	9.47	8.93	8.86	0.798	0.79
12 33 00.62	+27 42 44.8	−14.0	−14.0	0.0	0.0	10.42	9.80	9.47	8.94	8.87	0.805	0.79
12 35 17.03	+26 03 21.8	−2.0	−10.0	0.0	0.0	10.69	10.35	9.51	9.01	8.93	0.818	0.64
12 25 10.14	+27 39 44.8	−6.0	−12.0	0.0	0.0	10.69	10.10	9.57	9.07	8.93	0.777	0.79
12 18 57.27	+25 53 11.1	−12.0	−12.0	3.0	1.0	10.80	10.30	9.64	9.08	8.94	0.728	0.79
12 21 15.63	+26 09 14.1	−10.0	−8.0	0.0	0.0	10.87	10.41	9.62	9.09	8.97	0.773	0.79
12 32 08.09	+28 54 06.5	−10.0	−4.0	0.0	0.0	10.74	10.30	9.62	9.09	8.99	0.785	0.79
12 12 53.23	+26 15 01.3	−12.0	−12.0	0.0	0.0	10.54	9.72	9.58	9.11	8.99	0.819	0.64
12 23 47.23	+23 14 44.3	−12.0	−16.0	0.0	0.0	10.36	9.54	9.68	9.13	9.02	0.759	0.79
12 18 17.77	+23 38 32.8	−6.0	−14.0	0.0	0.0	10.77	10.28	9.76	9.20	9.10	0.759	0.79
12 22 52.37	+26 38 24.2	−8.0	−10.0	0.0	0.0	11.42	11.12	9.78	9.26	9.11	0.756	0.79
12 26 51.03	+26 16 01.9	−14.0	−2.0	0.0	0.0	11.07	10.56	9.85	9.27	9.16	0.725	0.79
12 09 12.44	+26 39 38.9	−16.0	−6.0	0.0	0.0	10.60	9.78	9.83	9.27	9.18	0.770	0.79
12 27 00.81	+29 36 37.9	−4.0	−6.0	0.0	0.0	11.07	10.70	9.80	9.33	9.20	0.806	0.79
12 23 28.21	+25 53 39.9	−10.0	−12.0	1.0	1.0	11.43	11.00	9.92	9.35	9.26	0.758	0.79
12 24 10.37	+29 29 19.6	−6.0	−2.0	0.0	0.0	10.77	10.27	10.06	9.50	9.33	0.683	0.79
12 34 46.93	+24 09 37.7	−12.0	−4.0	2.0	5.0	11.38	10.87	10.06	9.53	9.39	0.749	0.79
12 15 34.01	+26 15 42.9	−12.0	−6.0	0.0	0.0	11.08	10.26	10.13	9.57	9.47	0.757	0.79
12 26 00.26	+24 09 20.9	−10.0	−4.0	2.0	2.0	13.85	12.51	10.98	10.36	10.14	0.558	0.80
12 28 57.67	+27 46 48.4	−14.0	−2.0	3.0	2.0	13.04	11.37	10.99	10.35	10.19	0.552	0.80
12 16 00.86	+28 05 48.1	−12.0	−4.0	2.0	2.0	14.15	11.43	11.07	10.52	10.24	0.543	0.80
12 30 57.39	+22 46 15.2	−12.0	−4.0	3.0	1.0	14.37	12.13	11.24	10.65	10.42	0.514	0.80
12 31 57.42	+25 08 42.5	−10.0	−12.0	0.0	1.0	14.22	12.94	11.40	10.79	10.55	0.492	0.80
12 31 27.72	+25 23 39.9	−8.0	−6.0	1.0	2.0	14.07	12.96	11.44	10.84	10.63	0.478	0.80
12 25 55.76	+29 07 38.3	−8.0	−18.0	2.0	3.0	13.81	11.78	11.56	10.95	10.75	0.460	0.80
12 23 55.53	+23 24 52.3	−10.0	−4.0	1.0	0.0	14.37	12.64	11.59	10.99	10.77	0.455	0.80
12 25 02.64	+26 42 38.4	−8.0	−4.0	0.0	3.0	14.22	11.85	11.62	11.03	10.79	0.452	0.80
12 30 04.87	+24 02 33.9	−10.0	−8.0	3.0	0.0	14.76	13.27	11.77	11.18	10.94	0.428	0.80
12 18 12.77	+26 49 15.6	−8.0	0.0	1.0	1.0	15.61	12.78	12.02	11.46	11.15	0.392	0.60
12 15 16.93	+28 44 50.0	−12.0	−14.0	4.0	1.0	14.11	0.0	12.00	11.35	11.17	0.389	0.60
12 23 12.03	+23 56 15.1	−8.0	−6.0	2.0	1.0	15.40	13.31	12.20	11.61	11.38	0.352	0.60
12 31 00.28	+26 56 25.1	−16.0	−14.0	3.0	1.0	14.04	12.52	12.25	11.56	11.39	0.351	0.60
12 33 31.35	+24 12 09.1	−4.0	−16.0	1.0	2.0	14.76	13.45	12.29	11.59	11.40	0.348	0.60
12 16 37.30	+26 53 58.2	−10.0	−6.0	2.0	3.0	15.13	12.94	12.23	11.68	11.42	0.346	0.60
12 24 10.89	+23 59 36.4	−6.0	−4.0	4.0	1.0	15.60	13.67	12.27	11.66	11.45	0.340	0.60
12 28 38.70	+25 59 13.0	−6.0	−2.0	1.0	2.0	14.31	13.94	12.36	11.69	11.53	0.326	0.60
12 16 22.84	+24 19 01.1	−12.0	−2.0	2.0	4.0	14.78	13.96	12.39	11.73	11.55	0.323	0.60
12 27 08.56	+27 01 22.9	−16.0	−2.0	2.0	3.0	14.14	12.52	12.38	11.73	11.57	0.319	0.60
12 28 04.54	+24 21 07.6	−12.0	−10.0	1.0	3.0	15.75	14.29	12.39	11.84	11.58	0.318	0.60
12 38 04.72	+25 51 18.5	−16.0	−6.0	4.0	0.0	14.96	13.43	12.46	11.84	11.64	0.308	0.60
12 14 19.78	+25 10 46.6	−6.0	−12.0	3.0	3.0	14.81	13.92	12.50	11.80	11.65	0.305	0.60
12 28 50.08	+27 17 41.7	−20.0	−12.0	1.0	2.0	14.46	12.84	12.55	11.84	11.70	0.297	0.60
12 36 34.30	+25 00 38.3	−14.0	−2.0	4.0	6.0	15.59	13.43	12.51	11.96	11.70	0.298	0.60
12 26 37.32	+22 34 53.4	−12.0	−8.0	1.0	1.0	15.19	13.34	12.60	11.97	11.77	0.288	0.60
12 33 30.31	+28 12 55.9	−12.0	−14.0	2.0	11.0	14.06	13.59	12.65	12.07	11.84	0.279	0.60
12 16 29.21	+23 32 32.9	−12.0	−8.0	6.0	1.0	15.08	14.55	12.77	12.13	11.91	0.270	0.60
12 30 46.17	+23 45 49.0	−10.0	−6.0	1.0	9.0	15.43	13.83	12.72	12.17	11.91	0.269	0.60
12 19 37.99	+26 34 44.7	−6.0	−8.0	4.0	2.0	16.46	14.03	12.78	12.24	11.92	0.269	0.60
12 14 23.97	+28 21 16.6	−4.0	−8.0	2.0	1.0	15.52	0.0	12.83	12.14	11.92	0.269	0.60

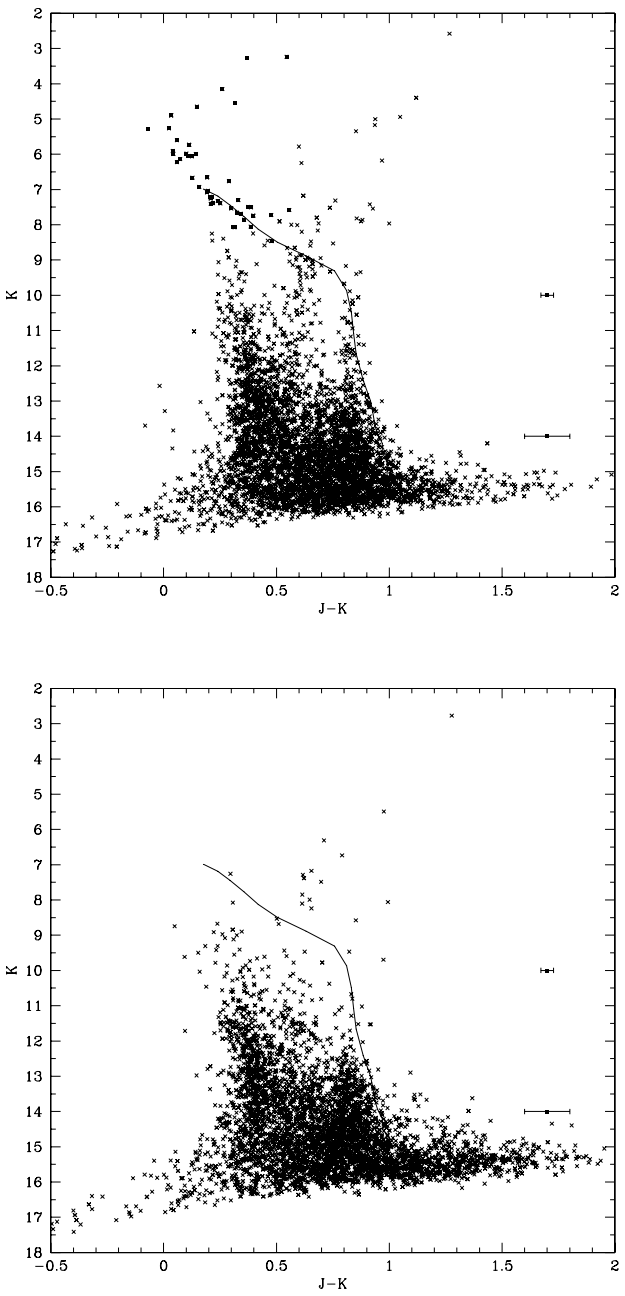

Figure 2. The CMD for the cluster (top) and a control sample with $\mu_\alpha = +11.21$, $\mu_\delta = -9.16$ (bottom). Previously known members of the cluster are highlighted in the upper plot (solid squares). A 0.4-Gyr NEXTGEN isochrone is overplotted from Baraffe et al. (1998) (solid line). This was converted into the 2MASS system using the transforms of Carpenter (2001).

the magnitude range where they overlap, the previously known cluster members of the single star sequence congregate around the theoretical isochrone (all previously known cluster members are listed in Table 1). Furthermore, the model isochrone appears to continue to follow closely the excess of objects in the top panel of Fig. 2, relative to the bottom panel, suggesting that it is relatively robust in this effective temperature regime.

The location of the theoretical isochrone at $J - K_S < 0.8$ is insensitive to the uncertainties in the age of the cluster. The cluster would have to be much younger to shift the isochrone significantly. The bulk of the observed dispersion in the single star sequence here probably stems from the finite depth of the cluster (∼0.15 mag). Nevertheless, in this colour range we choose to select objects that lie no more than 0.3 mag below the theoretical isochrone, as this ensures that all previously known cluster members are recovered (filled squares in Fig. 2, top panel). As binary members can lie up to 0.75 mag above the single star sequence, only objects that also lie no more than 1.05 mag above the theoretical sequence are deemed candidate members.

Redward of $J - K_S = 0.8$, the main sequence becomes very steep in this CMD. We have tried using various combinations of 2MASS and USNO-B1.0 photometry (e.g. colours such as $R - K$) to circumvent this. However, as mentioned previously, the poorer quality of the photographic magnitudes provided by the USNO-B1.0 catalogue results in a large amount of scatter in optical + infrared CMDs, rendering them of little use for this work. None the less, the finite depth of the cluster and a small error in cluster distance determination have a negligible effect in this part of the $J - K_S$, K_S CMD. Based on previous experience gained from our investigations of the low-mass members of the Pleiades and Praesepe open clusters, we estimate an uncertainty in the model $J - K$ colour of ±0.05 mag. Hence for $J - K_S > 0.8$ we have selected all objects that overlap a region 0.1 mag wide in $J - K$, centred on the theoretical isochrone.

To assess levels of contamination in our list of candidate members, we have imposed these same colour selection criteria on the control samples. The resulting sequences were divided into 1-mag bins (in K_S) for $J - K_S > 0.8$, and in bins of 0.2 in $J - K_S$ for $J - K_S < 0.8$, and the number of objects in each for both the cluster and control samples counted. Subsequently, the membership probablility for each candidate cluster member, $P_{\rm membership}$, was estimated using

$$P_{\rm membership} = \frac{N_{\rm cluster} - N_{\rm control}}{N_{\rm cluster}}, \quad (1)$$

where $N_{\rm cluster}$ is the number of stars in a magnitude bin from the cluster sample and $N_{\rm control}$ is the mean number of stars in the same magnitude range but drawn from the control samples. Our list of candidate associates of Melotte 111 is presented in Table 2, along with these estimates of membership probability.

We note that there is a slight increase in the level of contamination in the range $0.55 < J - K_S < 0.7$. A similar increase in the number of field stars was seen by Adams et al. (2002) when studying the Praesepe open cluster, which, like Melotte 111, has a relatively high Galactic latitude, $b = 38°$. We believe that this is due to K giants located in the thick disc.

3 RESULTS

Our survey of the Coma Berenices open cluster has recovered 45 previously known members in total, 38 listed by Bounatiro & Arimoto (1993) and seven unearthed by Odenkirchen et al. (1998). Furthermore, it has identified 60 new candidate cluster members with magnitudes down to $K_S = 12$. Beyond this magnitude, no statistically significant difference between the cluster and the control samples was found, as the contamination by field stars is too great. We believe that our survey is reasonably complete to this limit; we tried proper motion search radii of 7 and 5 mas yr^{-1}, but in both cases found that increasing numbers of likely members were excluded. Expanding the search radius to greater than 10 mas yr^{-1} unearthed no statistically significant increase in the number of candidate members, as the candidates and control stars increased proportionally, leading to many candidates with extremely small probabilities of being cluster members. Our survey is complete to 90 per cent at this

radius, as explained earlier. As the stars get fainter, however, the errors in their proper motion do increase – which is to be expected. It is entirely possible that the completeness is less than 90 per cent for the faint stars.

We have estimated the masses of our candidates and the previously known cluster members using the evolutionary tracks of Girardi et al. (2002) for masses $\geqslant 1\,M_{\odot}$, and the NEXTGEN models of Baraffe et al. (1998) for $M < 1\,M_{\odot}$. The stars were binned according to K magnitude or $J - K$ colour, for the vertical and diagonal portions of the main sequence. We then linearly interpolated between the model masses to estimate the masses of the cluster stars and our candidates. These masses are shown in the final columns of Tables 1 and 2, and illustrated in Fig. 5 (later). By multiplying the estimated masses of the stars by their membership probabilities (we assume $P_{\rm membership} = 1.0$ for previously known members) and summing, we determine a total cluster mass of $\sim 102\,M_{\odot}$. This in turn allows us to derive a tidal radius of 6.5 pc or $4\overset{\circ}{.}1$ at 90 pc. Thus we find that within our adopted survey radius of 4° we should expect to find 99 per cent of the gravitationally bound proper motion selected cluster members. Indeed, increasing the search radius to 5° led to a near-equal increase in both candidate cluster members and stars in the control.

Fig. 3 shows the $H - K$, $J - H$ two-colour diagram for all new candidate and previously known cluster members. The colours of our candidates show a clear turnover at $H - K \approx 0.15$, consistent with them being dwarfs and supporting our conclusion that these are low-mass members of Melotte 111. Therefore we have constructed a $K_{\rm S}$ luminosity function and mass function for the cluster (Figs 4 and 5). The luminosity function is seen to peak at $K_{\rm S} = 7.5$, $M_{K_{\rm S}} = 2.7$ and to decline gradually towards fainter magnitudes. Superimposed on this decline is the Wielen dip (Wielen 1971) at $K_{\rm S} = 10.5$.

The peaking of the luminosity function at this comparatively bright magnitude strongly suggests that a large proportion of the lower mass members, which are normally more numerous than the higher mass members (e.g. Hambly, Hawkins & Jameson 1991), have evaporated from the cluster. This should not come as a great surprise, since at ages $\tau \gtrsim 200$ Myr dynamical evolution of a typical open cluster is expected to lead to the loss of a significant and increasing fraction of the lowest mass members (e.g. de la Fuente Marcos & de la Fuente Marcos 2000). The mass function also supports this conclusion. Thus, despite having found low-mass stars in the cluster, our study does not contradict the conclusion of previous authors that the cluster is deficient in low-mass stars. Odenkirchen et al. (1998) found that the luminosity function of extra-tidal stars

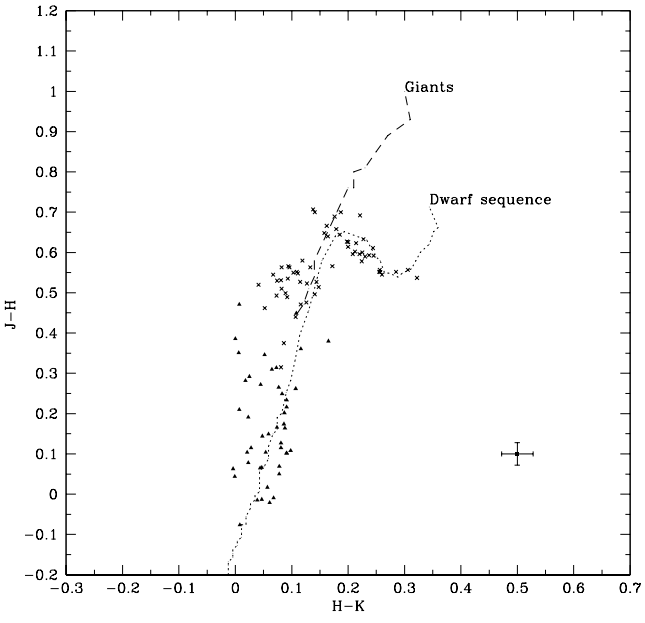

Figure 3. A *JHK* colour–colour diagram for candidate (crosses) and previously known (solid triangles) cluster members. Empirical dwarf (dotted line) and giant (dashed line) sequences of Koornneef (1983) are overplotted. The diagram has been plotted using the 2MASS system. The colour transformations of Carpenter (2001) were used to convert the model colours.

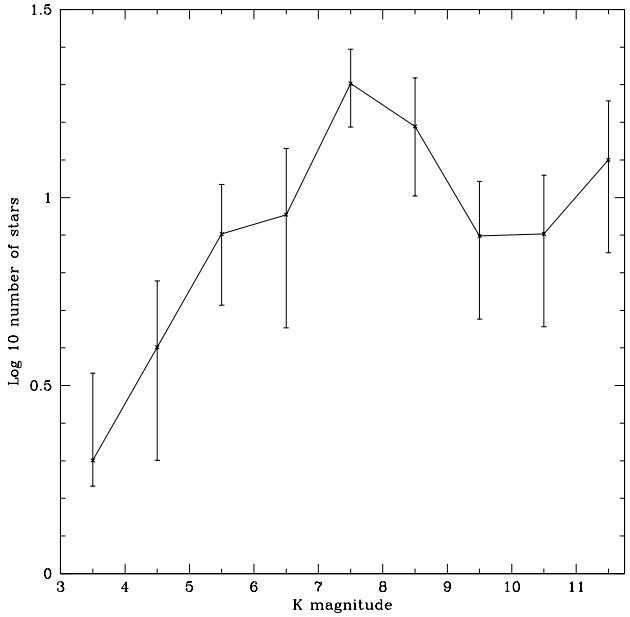

Figure 4. Luminosity function for the cluster, taking into account probability of membership. The error bars indicate the Poisson error.

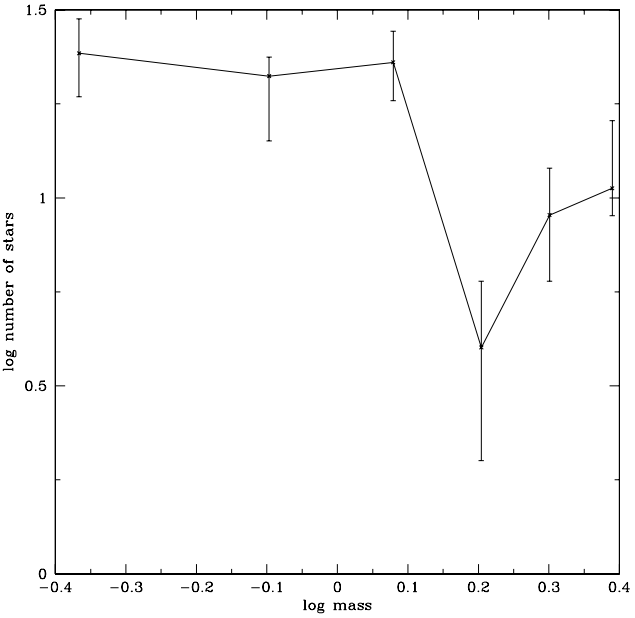

Figure 5. Mass function for the cluster, taking into account probability of membership. The error bars indicate the Poisson error.

associated with the cluster rises towards lower masses. This can be considered to be indicative of the ongoing loss of low-mass members. Ford et al. (2001), however, determined that approximately half of these stars did not belong to the cluster. A more in-depth study of lower mass members would be required to determine a more accurate luminosity function at fainter magnitudes.

Our faintest candidate member has an estimated mass of $0.269\,M_{\odot}$. There are some 18 stars in the magnitude range $K_S = 11$–12, the lowest luminosity bin, thus it seems a distinct possibility that the Coma Berenices open cluster will have members right down to the limit of the hydrogen-burning main sequence and possibly into the brown dwarf regime. This conclusion is also confirmed by the rising mass function at lower masses.

4 CONCLUSIONS

We have performed a deep, wide-area survey of the Coma Berenices open star cluster, using the USNO-B1.0 and the 2MASS Point Source catalogues, to search for new candidate low-mass members. This has led to the identification of 60 objects with probabilities of cluster membership $P_{\rm membership} \gtrsim 0.6$. Our lowest mass new candidate member has $M \approx 0.269\,M_{\odot}$, in contrast to the previously known lowest mass member, $M \approx 0.915\,M_{\odot}$. Thus we have extended considerably the cluster luminosity function towards the bottom of the main sequence. As reported by previous investigations of Melotte 111, the luminosity function is observed to decline towards fainter magnitudes, indicating that the cluster has probably lost and continues to lose its lowest mass members. This is not surprising for a cluster with an age of 400–500 Myr. Nevertheless, as the cluster luminosity function remains well above zero at $K_S = 12$, we believe that the cluster probably has members down to the bottom of the hydrogen-burning main sequence and possibly some brown dwarfs. Thus a deeper *IZ* magnitude survey of the cluster could prove a fruitful undertaking.

ACKNOWLEDGMENTS

This research has made use of the USNOFS Image and Catalogue Archive operated by the United States Naval Observatory, Flagstaff Station (http://www.nofs.navy.mil/data/fchpix/). This publication has also made use of data products from the Two-Micron All-Sky Survey, which is a joint project of the University of Massachusetts and the Infrared Processing and Analysis Center/California Institute of Technology, funded by the National Aeronautics and Space Administration and the National Science Foundation. SLC and PDD acknowledge funding from PPARC.

REFERENCES

Adams J. D., Stauffer J. R., Skrutskie M. F., Monet D. G., Portegies Zwart S. F., Janes K. A., Beichman C. A., 2002, AJ, 124, 1570
Argue A. N., Kenworthy C. K., 1969, MNRAS, 146, 479
Artyukhina N. M., 1955, Trudy Gosudarstvennogo Astron. Inst., 26, 3
Baraffe I., Chabrier G., Allard F., Hauschildt P. H., 1998, A&A, 337, 403
Bounatiro L., Arimoto N., 1993, A&A, 268, 829
Bouvier J., Stauffer J. R., Martin E. L., Barrado y Navascues D., Wallace B., Bejar V. J. S., 1998, A&A, 336, 490
Carpenter J. M., 2001, AJ, 121, 2851
Cayrel de Strobel G., 1990, Soc. Astron. Italiana Mem., 61, 613
de la Fuente Marcos R., de la Fuente Marcos C., 2000, Ap&SS, 271, 127
Deluca E. E., Weis E. W., 1981, PASP, 93, 32
Ford A., Jeffries R. D., James D. J., Barnes J. R., 2001, A&A, 369, 871
Friel E. D., Boesgaard A. M., 1992, ApJ, 387, 107
Garcia-Lopez R. J., Randich S., Zapatero Osorio M. R., Pallavicini R., 2000, A&A, 363, 958
Girardi L., Bertelli G., Bressan A., Chiosi C., Groenwegen M. A. T., Marigo P., Salasnich B., Weiss A., 2002, A&A, 391, 195
Gizis J. E., Reid I. N., Monet D. G., 1999, AJ, 118, 997
Hambly N. C., Hawkins M. R. S., Jameson R. F., 1991, MNRAS, 253, 1
Jameson R. F., Skillen I., 1989, MNRAS, 239, 247
Koornneef J., 1983, A&A, 128, 84
Lodieu N., McCaughrean M. J., Barrado y Navascus D., Bouvier J., Stauffer J. R., 2005, A&A, 436, 853
Madsen S., Dravins D., Lindgren L., 2002, A&A, 381, 446
Monet D. G. et al., 2003, ApJ, 125, 984
Moraux E., Bouvier J., Stauffer J. R., 2001, A&A, 367, 211
Nicolet B., 1981, A&A, 104, 185
Odenkirchen M., Soubiran C., Colin J., 1998, New Astron., 3, 583
Oort J. H., 1979, A&A, 78, 312
Perryman M. A. C. et al., 1998, A&A, 331, 81
Randich S., Schmitt J. H. M. M., Prosser C., 1996, A&A, 313, 815
Reid I. N., 1992, MNRAS, 257, 257
Reid I. N., 1993, MNRAS, 265, 785
Skrutskie M. F. et al., 1997, in Garzon F. et al., eds, The Impact of Large Scale Near-IR Sky Surveys. Kluwer, Dordrecht, p. 25
Trumpler R. J., 1938, Lick Obs. Bull., 18, 167
Tsvetkov T. G., 1989, Ap&SS, 151, 47
van Leeuwen F., 1999, A&A, 341, L71
Wielen R., 1971, A&A, 13, 309
Zacharias N., Urban S. E., Zacharias M. I., Wycoff G. L., Hall D. M., Monet D. G., Rafferty T. J., 2004, AJ, 127, 3043

This paper has been typeset from a TEX/LATEX file prepared by the author.